horticulturae

MDPI

Article

Pre-Harvest Bagging Induces Consistent Biomechanical Softening and Highly Plastic Colorimetric Responses in Table Grapes During an Extreme Heatwave Season

Nataly Tatiana Coronel Montesdeoca [1,*], Esther Sendra [2] and Francisca Hernández [3,*]

[1] Grupo de Investigación Agricultura Sostenible (GIAS), Carrera de Agropecuaria, Universidad Politécnica Estatal del Carchi, Tulcán 040102, Ecuador
[2] Research Group "Food Quality and Safety", Institute for Agri-Food and Agri-Environmental Research and Innovation, Miguel Hernández University (CIAGRO-UMH), 03312 Alicante, Spain; esther.sendra@umh.es
[3] Research Group in Fruit Science and Production Techniques, Institute for Agri-Food and Agri-Environmental Research and Innovation, Miguel Hernández University (CIAGRO-UMH), Ctra. Beniel, km 3,2, 03312 Alicante, Spain
* Correspondence: nataly.coronel@upec.edu.ec (N.T.C.M.); francisca.hernandez@umh.es (F.H.)

Abstract

Global warming and extreme radiation compromise the quality of table grapes (*Vitis vinifera* L.). Although preharvest bagging mitigates heat stress, the stability of its effect on overall quality in the face of interannual climate variability remains poorly understood. The objective was to determine the independent and interactive effects of light exclusion, cultivar, and season on epidermal biomechanics, color, and technological maturity. A 2 × 2 × 2 orthogonal factorial design was implemented, evaluating two cultivars ("Aledo" and "Doña María"), two microclimates (cellulose bag vs. uncovered), two consecutive seasons (a standard historical cycle in 2022 versus an extreme heatwave anomaly in 2023). Physical and chemical parameters were evaluated (a total of 480 analytical subsamples (berries) were collapsed into N = 24 true experimental units (clusters) for all inferential and multivariate analyses). Principal Component Analysis (PCA) captured 71% of the total variance, revealing opposing driving vectors. Bagging significantly reduced the maximum epidermal puncture force ($F = 51.46$, $p < 0.001$), exhibiting a consistent directional response, with no significant interactions with genotype or year. In contrast, primary metabolism exhibited high plasticity; the technological maturity index (TSS/Acidity) revealed highly significant third-order interactions ($F = 58.67$, $p < 0.001$), indicating a marked genotypic and climatic dependence. Microclimate modification exerts a strong buffering effect: it consistently reduces the biomechanics of the epidermis (firmness), but both the colorimetric phenotype (L^*, a^*) and the internal ripening dynamics (Maturity Index) remain highly plastic and sensitive to environmental fluctuations, requiring crop-specific agronomic management.

Keywords: *Vitis vinifera* L.; thermal stress; cluster bagging; microclimate; technological maturity; epidermal biomechanics; CIELAB color space; climate resilience

Check for updates

Academic Editors: Xiaolin Yu and Zhenfeng Yang

Received: 22 September 2026
Revised: 4 November 2026
Accepted: 16 November 2026
Published: 18 November 2026

Copyright: © 2026 by the authors. Licensee MDPI, Basel, Switzerland. This article is an open access article distributed under the terms and conditions of the Creative Commons Attribution (CC BY) license.

1. Introduction

Table grapes (*Vitis vinifera* L.) have established themselves as one of the most valuable fruit crops on the international market, accounting for a substantial portion of global fruit production and serving as a vital source of nutraceuticals, bioactive compounds, and functional lipids [1,2]. However, in the current context of climate change, high temperatures and excessive solar radiation during the ripening period seriously compromise the quality of the

fruit [3,4]. Severe heat stress accelerates malic acid respiration, raising the pH and altering technological ripeness to the detriment of color ripeness. As a cellular defense mechanism to maintain integrity against heat and prevent physical damage such as sunburn, the berries undergo critical changes in the architecture of their cell walls and in the dynamics of sugar accumulation, which directly impacts skin firmness and technological maturity [1,5].

To mitigate the effects of abiotic and biotic stress, various techniques have been developed to protect the grape cluster, with individual preharvest bagging being one of the most widely used agronomic practices worldwide [6,7]. Traditionally, this physical barrier, along with the use of protective netting, has been implemented to moderate leaf temperature during extreme weather events and reduce the incidence of chemical residues in a sustainable manner [8,9].

Despite its extensive agronomic benefits, various authors have measured the effects of bagging on fruit quality, yielding results that are highly dependent on the genotype and the growing environment [10,11]. For example, in specific table grape cultivars, it has been reported that the metabolic modulation of fatty acids induced by the bag is strictly cultivar-specific [1]. Even more critically, longitudinal studies have shown that the accumulation of flavonoids, hydroxybenzoic acids, and anthocyanins under light exclusion is inconsistent from year to year, varying dramatically due to subtle interannual weather fluctuations [5,10]. In trials with Muscat cultivars, changes in the microclimate significantly altered the sugar-to-acid ratio in some varieties, while in others it had no effect at all [11].

At the cellular level, heat and excess light stress trigger reactive oxygen species (ROS) accumulation, redox imbalance, stress granule dynamics, and reprogramming of carbon partitioning. These processes influence sugar accumulation, organic acid turnover, and secondary metabolism, and therefore affect total soluble solids (TSS), titratable acidity (TA), and color development. Recent studies have demonstrated that precision engineering of carbon partitioning can enhance crop resilience to heat stress [12], that stress granule dynamics are central to high-temperature survival [13], and that ROS-scavenging modules regulate acclimation to excess light [14]. This mechanistic framework is largely missing from the table grape bagging literature and helps explain the physiological rationale behind bagging-induced phenotypic stabilization.

In recent years, various studies have sought to explain the molecular and environmental causes of this phenotypic plasticity; however, the stability of bagging-induced modulation across different genotypes and highly unstable climatic cycles remains poorly understood. Consequently, to address this gap in the literature, the objective of this study was to determine the independent and interactive effects of microclimate modification, cultivar, and harvest season on the epidermal firmness and colorimetric parameters of table grapes.

2. Materials and Methods

2.1. Plant Material and Experimental Design

The experiment was conducted over two consecutive growing seasons (2022 and 2023) in commercial vineyards located in Novelda (Alicante, Spain; UTM ETRS89 coordinates 30N, X: 695,138, Y: 4,252,647), a region characterized by its semi-arid Mediterranean climate [8], within the production area of the Protected Designation of Origin (PDO) "Uva de Mesa Embolsada del Vinalopó" [1]. Mature vines (approximately 10 years old) grafted onto 140 Ruggeri (140 Ru) rootstocks and trained on a traditional Spanish parral (overhead pergola) trellis system with a NW–SE (Northwest–Southeast) row orientation and a planting spacing of 2.0 × 2.5 m were selected [1,8]. Two table grape cultivars (*Vitis vinifera* L.) were evaluated: 'Aledo' and 'Doña María'. The experiment was structured as a 2 × 2 × 2 orthogonal factorial design (Cultivar × Microclimate × Year) arranged in a Completely Randomized Design (CRD). Following the exact sampling framework described in Andreu-

Coll et al. [15], thirty clusters ($n = 30$) were harvested per treatment group, with unbagged control fruit sourced from other commercial farms in the region. To perform the rigorous physicochemical assessments, these 30 clusters were randomly pooled into three composite biological replicates (10 clusters per pool). Therefore, the statistical experimental unit for all inferential models is the composite pool ($n = 3$ per treatment group, N = 24 total experimental units). Crucially, to ensure strict comparability across seasons, the 2023 extreme heatwave experimental trial was designed to exactly replicate the 2022 baseline sampling protocol (e.g., identical sample size of $n = 30$, identical PDO commercial harvest criteria, and congruent analytical methods.

Agronomic management practices were kept identical across all experimental plots. The vineyard was managed under standard commercial drip irrigation, receiving approximately 4000 m^3/ha/year with watering frequency dynamically adjusted to atmospheric demand to prevent severe water deficit during the heatwaves. Standard fertilization protocols (100 kg N, 50 kg P_2O_5, and 140 kg K_2O per hectare) were applied uniformly across both seasons [1,8].

2.2. Light-Exclusion Treatments (Bagging)

The microclimate modification treatment consisted of bagging individual grape clusters located consistently on the middle canes of the canopy to ensure uniform basal sunlight exposure prior to treatment. In August of each growing season, coinciding exactly with phenological stage BBCH 81 (veraison: the onset of ripening, when the berries begin to take on a glossy sheen), the selected clusters were covered with protective bags. In strict compliance with the regulatory standards of the Vinalopó PDO, long-fiber cellulose bags treated with melamine for moisture resistance were used; these bags had a satin finish, a cane-colored appearance, and a standard weight of 40 g/m^2, dimensions of 26 × 40 cm (size No. 3), and an approximate PAR (400–700 nm) light transmittance of 50% (range: 45–55%). Bags remained on the clusters for a duration of up to 120 days until harvest and were removed immediately before sampling. Harvesting was performed manually according to the commercial criteria of the PDO [1]; the 'Doña María' variety (mid-season cycle) was harvested in the second week of October (resulting in a bagging duration of approximately 70–75 days), whereas the 'Aledo' variety (late cycle) was harvested in the last week of November (resulting in a bagging duration of approximately 120 days). This inherent difference in light-exclusion duration is intrinsically linked to the natural phenological ripening cycles of each cultivar.

2.3. Environmental Monitoring and Heat Stress Characterization

To accurately characterize the thermal severity and interannual climate variability in the semi-arid Mediterranean conditions of the Vinalopó region, meteorological data were analyzed for the fruit development and ripening periods of both seasons. As detailed in recent regional monitoring for this specific vineyard location [1], the 2022 season closely followed standard historical conditions. In stark contrast, the 2023 season represented a statistically extreme anomaly characterized by severe heat stress. The August 2023 period experienced unprecedented heat waves, with maximum temperatures frequently exceeding 42 °C and peaking at 44.3 °C, coupled with a severe rainfall deficit. While microclimate parameters strictly inside the cellulose bags were not continuously monitored with data loggers in this specific trial, the macroscopic protective effect of light exclusion was evaluated directly through the biomechanical and metabolic responses of the berries.

2.4. Physicochemical and Colorimetric Analysis

To ensure robust biological representativeness and account for intra-cluster variability, a hierarchical sampling scheme was implemented. From each experimental unit (cluster), 20 berries were systematically collected from the upper, equatorial, and lower sections of the rachis as analytical subsamples [1]. Consequently, a total of 60 berries per treatment combination were evaluated for physical parameters, but their values were mathematically averaged prior to inferential analysis to avoid pseudoreplication. Individual weight was recorded using a precision analytical balance (BL-600, Sartorius, Madrid, Spain) [8,15]. The color profile was determined using a colorimeter (C-300 Chroma Meter, Minolta Corp., Osaka, Japan) [8], configured with a standard illuminant D65 and a 10° observer angle. A total of two readings per berry were taken around the equatorial zone of each berry, evaluating the CIE Lab* color space according to international standard parameters for color metrology in fruits [16]. Total soluble solids (TSS) were determined from the homogenized must extracted from the 20 analytical subsamples (berries) of each independent cluster. Measurements were performed using a digital refractometer (model N-20; Atago, Bellevue, WA, USA) at 20 °C, with results expressed in degrees Brix (°Brix). The specific standard deviation of 0.00 observed in certain subgroups reflects identical readings across the three biological replicates, driven exclusively by the zero-decimal resolution limit of the utilized refractometer, which masked subtle natural variations among the highly uniform pooled samples. Baseline primary metabolism data (TSS and TA) for the 2022 season cohorts were collected as part of a broader longitudinal monitoring program within the PDO region, with aggregate regional results previously reported in Andreu-Coll et al. [17]. Titratable acidity (TA) was quantified using an acid-base potentiometer (877 Titrino plus, Metrohm Ion Analysis CH9101, Herisau, Switzerland), employing 0.1 mol L^{-1} NaOH until a pH of 8.1 was reached. All analyses were performed in triplicate The technological maturity index was calculated as the ratio of total soluble solids (TSS, °Brix) to titratable acidity (TA, expressed as g tartaric acid/100 mL).

2.5. Instrumental Texture (Puncture Force)

The biomechanical strength of the epidermis (maximum puncture force) was assessed individually on whole berries using a texture analyzer (TX-XT2i Texture Analyzer, Stable Microsystems, Surrey, United Kingdom) [6]. Each berry underwent a puncture test at its equatorial region using an ebonite probe of 10 mm diameter (P10). The probe penetrated the skin to a depth of 5 mm at a constant test speed of 1.0 mm/s. This test was designed to accurately measure the maximum epidermal rupture force, with the final result expressed in grams of force (g).

2.6. Data Management and Statistical Analysis

Data management and inferential analysis were performed using the R programming environment, version 4.4.3 [18]. Prior to inference, matrix cleaning was performed to identify and correct implausible instrumental outliers. To strictly preserve the assumption of independence and avoid pseudoreplication, all subsample data collected at the berry level were averaged to calculate the cluster mean before inferential testing. Therefore, the three-way ANOVA and the multivariate Principal Component Analysis (PCA) were executed using the cluster as the sole experimental unit ($n = 3$ per group; total N = 24). A three-way ANOVA was used to evaluate main and interactive effects, with normality (Shapiro–Wilk) and homoscedasticity (Levene) tested using the car package [19].

To quantify the magnitude of the observed phenomena, effect sizes were calculated and reported as partial eta-squared (η_p^2). When significant interactions were detected, simple main effects were analyzed, and multiple comparisons were controlled using Tukey's Honestly Significant Difference (HSD) post hoc test multivariate variance was analyzed using Principal Component Analysis (PCA) with the FactoMineR software package (R version 4.4.1) [20]. Prior to averaging the subsamples, an exploratory data analysis was conducted at the berry level. One instrumental outlier in the 'Doña María' 2023 bagged cohort was identified (exceeding ±3 standard deviations from the mean due to a texture analyzer probe misfire) and subsequently excluded.

The true experimental unit (cluster) mean was calculated using the remaining valid subsamples, fully preserving the orthogonality of the experimental design (N = 24). To prevent structural redundancy and artificial collinearity, derived ratios (i.e., the Maturity Index) were strictly excluded from the multivariate matrix. Furthermore, 95% confidence ellipses were omitted from the visualization to avoid statistical over-interpretation due to the sample size ($n = 3$ clusters per group).

3. Results

3.1. Descriptive Analysis and Compliance with Parametric Assumptions

Prior to statistical inference, model assumptions were verified for each response variable. Levene's test confirmed homogeneity of variances for all variables (TSS: $p = 0.365$; TA: $p = 0.232$; MI: $p = 0.826$; firmness: $p = 0.799$). The Shapiro–Wilk test revealed a slight deviation from normality only for TSS ($p = 0.0004$), while TA ($p = 0.089$), MI ($p = 0.994$) and firmness ($p = 0.147$) satisfied the normality assumption. Given the balanced design ($n = 3$ clusters per treatment), the confirmed homoscedasticity, and the very large effect sizes obtained (partial $\eta^2 > 0.6$ for most factors), the parametric three-way ANOVA was retained as a robust analytical approach. The descriptive physicochemical parameters and technological maturity data are summarized in Table 1 and Table 2, respectively.

Table 1. Descriptive physicochemical parameters of the berry, categorized by cultivar, microclimate, and season.

Cultivar	Season	Microclimate	*n*	Maximum Puncture Force (g)	Berry Weight (g)
Aledo	2022	Bagged	60	296.32 ± 71.60 (c)	4.72 ± 1.00 (d)
		Uncovered	60	352.97 ± 76.66 (abc)	5.04 ± 1.02 (cd)
	2023	Bagged	60	331.23 ± 78.10 (bc)	4.48 ± 0.80 (d)
		Uncovered	60	400.29 ± 85.13 (a)	4.95 ± 0.75 (cd)
Doña María	2022	Bagged	60	252.41 ± 61.02 (c)	8.97 ± 1.32 (ab)
		Uncovered	60	341.29 ± 73.46 (bc)	7.08 ± 1.05 (bc)
	2023	Bagged	60	291.33 ± 63.40 (c)	10.16 ± 1.97 (a)
		Uncovered	60	369.34 ± 62.39 (ab)	9.16 ± 1.56 (ab)

Note: Values are expressed as Mean ± Standard Deviation (SD). The '$n = 60$' represents the total analytical subsamples (berries) measured per treatment. For statistical inference (ANOVA), these values were collapsed to $n = 3$ true experimental units (clusters) per group. Means followed by different letters within the same column indicate statistically significant differences according to Tukey's HSD test ($p < 0.05$).

Table 2. Descriptive parameters of technological maturity (primary metabolism) categorized by cultivar, microclimate, and season.

Cultivar	Season	Microclimate	TSS (°Brix)	TA (g Tartaric Acid/100 mL)	MI
Aledo	2022	Bagged	19.00 ± 0.00 (g)	0.33 ± 0.01 (d)	57.0 ± 1.0 (c)
		Uncovered	19.93 ± 0.29 (f)	0.38 ± 0.00 (c)	52.5 ± 1.1 (d)
	2023	Bagged	22.33 ± 0.06 (d)	0.52 ± 0.01 (a)	42.9 ± 1.1 (e)
		Uncovered	21.90 ± 0.00 (e)	0.54 ± 0.02 (a)	40.9 ± 1.3 (e)
Doña María	2022	Bagged	23.17 ± 0.06 (c)	0.33 ± 0.00 (d)	70.5 ± 0.9 (a)
		Uncovered	25.40 ± 0.53 (b)	0.46 ± 0.03 (b)	55.6 ± 2.4 (cd)
	2023	Bagged	25.03 ± 0.06 (b)	0.38 ± 0.01 (c)	65.7 ± 1.6 (b)
		Uncovered	27.73 ± 0.06 (a)	0.40 ± 0.00 (c)	69.9 ± 0.5 (a)

Note: Values are expressed as Mean ± Standard Deviation (SD). The '$n = 60$' analytical subsamples (berries) per treatment were collapsed to $n = 3$ true experimental units (clusters) prior to analysis. TSS = Total Soluble Solids; TA = Titratable Acidity; MI = TSS/TA. Means followed by different letters within the same column indicate statistically significant differences according to Tukey's HSD test ($p < 0.05$).

3.2. Main and Interactive Effects on Univariate Quality

The comprehensive ANOVA model (Table 3) showed that maximum puncture force (epidermal firmness) is strongly influenced by all three factors independently. The light-exclusion treatment exerted the absolute dominant main effect ($F = 51.46, p < 0.001$), with a massive effect size (partial $\eta^2 = 0.76$) indicating that microclimate modification drives the vast majority of texture variance. The factorial ANOVA confirmed the complete absence of significant interactions for texture ($p > 0.05$ for all interactive terms). Consequently, post hoc multiple comparisons were restricted to main effects, demonstrating that the softening induced by bagging is a consistent phenotypic response within the tested cultivars and seasons.

In contrast, primary metabolism exhibited highly interactive and genotype-dependent behavior. Descriptive data for these technological maturity parameters are presented in Table 2, while the inferential models (Table 3) revealed highly significant third-order interactions (Cultivar × Microclimate × Season) for TSS ($F = 26.77$, $p < 0.001$, $\eta^2p = 0.63$), TA ($F = 14.77$, $p = 0.001$, $\eta^2p = 0.48$), and Maturity Index ($F = 58.67$, $p < 0.001$, $\eta^2p = 0.79$). Notably, the main effect of cultivar dominated both TSS ($\eta^2p = 0.99$) and MI ($\eta^2p = 0.98$), whereas season was the strongest driver of TA ($\eta^2p = 0.94$). Microclimate also showed large main effects on all three variables (TSS: $\eta^2p = 0.94$; TA: $\eta^2p = 0.85$; MI: $\eta^2p = 0.80$). This hierarchy of effect sizes demonstrates that the magnitude and direction of metabolic decoupling are determined simultaneously by genetic background and the thermal severity of the cycle, with the triple interaction retaining substantial biological relevance across all primary-metabolism traits.

To unravel these third-order interactions, simple main effects were analyzed, and interaction plots were generated (Figure 1). The post hoc Tukey HSD comparisons are represented by letters above each point in Figure 1, confirming that the environmental buffering effect of the bag on primary metabolism is highly cultivar-specific.

Table 3. Analysis of variance (three-way ANOVA) for the main and interactive effects of cultivar, microclimate, and season on epidermal firmness and technological ripeness.

Source of Variation	df	Firmness (g Force)			TSS (°Brix)			TA (g Tartaric Acid/100 mL)			MI		
		F	p	η_p^2	F	p	η_p^2	F	p	η_p^2	F	p	η_p^2
Main Effects													
Cultivar (Aledo vs. Doña María)	1	9.61	0.007	0.38	2628.54	<0.001	0.99	90.70	<0.001	0.85	984.58	<0.001	0.98
Microclimate (Bagged vs. Uncovered)	1	51.46	<0.001	0.76	235.12	<0.001	0.94	91.29	<0.001	0.85	62.14	<0.001	0.80
Season (2022 vs. 2023)	1	13.38	0.002	0.46	718.80	<0.001	0.98	239.70	<0.001	0.94	54.45	<0.001	0.77
Interactions													
Cultivar × Microclimate	1	1.02	0.328	0.06	156.54	<0.001	0.91	14.54	0.002	0.48	3.54	0.078	0.18
Cultivar × Season	1	0.14	0.713	0.01	9.64	0.007	0.38	264.19	<0.001	0.94	258.82	<0.001	0.94
Microclimate × Season	1	0.001	0.970	0.00	6.45	0.022	0.29	44.67	<0.001	0.74	97.95	<0.001	0.86
Cultivar × Microclimate × Season	1	0.33	0.576	0.02	26.77	<0.001	0.63	14.77	0.001	0.48	58.67	<0.001	0.79
Residual error	16	-	-	-	-	-	-	-	-	-	-	-	-

Note: df = degrees of freedom; F = Fisher's statistic; p = significance level; η_p^2 = partial eta-squared (effect size). The Maturity Index was calculated as the ratio of Total Soluble Solids to Titratable Acidity.

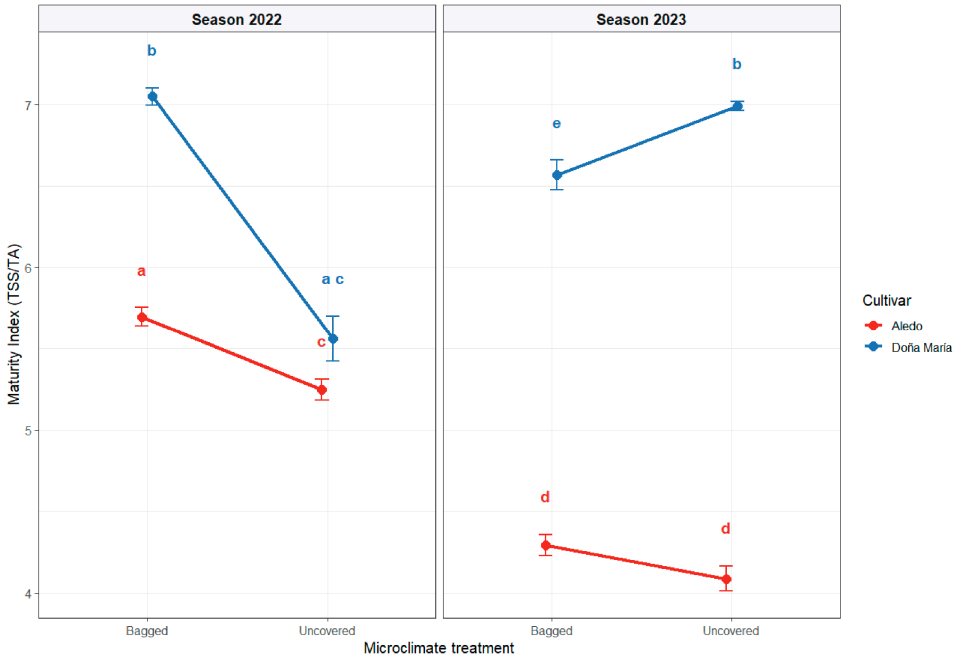


Figure 1. Interaction plots illustrating the third-order interactive effect (Cultivar × Microclimate × Season) on the technological Maturity Index (TSS/TA) of table grapes. The graphs demonstrate the high plasticity of primary metabolism, where the magnitude of the bagging effect is strictly dependent on the genotype and the thermal severity of the year. Error bars represent the standard error of the mean (n = 3 clusters per experimental unit).

To support the visual findings and address the plasticity of the epidermal color, a univariate analysis was performed on the CIELAB color space coordinates, Chroma, and Hue angle (Table 4). Contrary to the biomechanical firmness, the independent main effect of the bagging treatment was not statistically significant for Lightness (L^*, $p = 0.110$), a^* ($p = 0.611$), or Chroma ($p = 0.063$). Instead, the colorimetric expression was heavily governed by significant third-order interactions (Cultivar × Microclimate × Season) for L^* ($p = 0.025$), a^* ($p < 0.001$), and Hue angle ($p < 0.001$). This indicates that while the bag acts as a physical barrier, its specific modulation of the grape's color profile is not universal; it is highly plastic and strictly dependent on the underlying genotype and the thermal severity of the harvest year."

Table 4. Analysis of variance (three-way ANOVA) for the main and interactive effects of cultivar, microclimate, and season on CIELAB colorimetric coordinates, Chroma, and Hue angle.

Source of Variation	df	L^* (Lightness)			a^* (Red/Green)			B^* (Yellow/Blue)			Chroma			Hue Angle		
		F	***p***	η_p^2	***F***	***p***	η_p^2	***F***	***p***	η_p^2	***F***	***p***	η_p^2	***F***	***p***	η_p^2
Main Effects																
Cultivar	1	380.96	<0.001	0.96	18.07	<0.001	0.53	7.79	0.013	0.33	4.73	0.045	0.23	22.20	<0.001	0.58
Microclimate	1	2.86	0.110	0.15	0.27	0.611	0.02	3.41	0.083	0.18	3.99	0.063	0.20	1.96	0.180	0.11
Season	1	453.86	<0.001	0.97	31.33	<0.001	0.66	107.26	<0.001	0.87	114.91	<0.001	0.88	0.01	0.937	0.00
Interactions																
Cultivar × Microclimate	1	0.27	0.613	0.02	14.53	0.002	0.48	0.41	0.533	0.03	1.20	0.289	0.07	7.86	0.013	0.33
Cultivar × Season	1	4.31	0.054	0.21	4.23	0.056	0.21	23.65	<0.001	0.60	19.73	<0.001	0.55	10.83	0.005	0.40
Microclimate × Season	1	7.13	0.017	0.31	31.03	<0.001	0.66	1.18	0.293	0.07	0.13	0.722	0.01	41.45	<0.001	0.72
Cultivar × Microclimate × Season	1	6.15	0.025	0.28	25.63	<0.001	0.62	0.20	0.661	0.01	1.13	0.304	0.07	17.36	<0.001	0.52

Note: df = degrees of freedom; F = Fisher's statistic; p = significance level; η_p^2 = partial eta-squared (effect size). The Maturity Index was calculated as the ratio of Total Soluble Solids to Titratable Acidity.

3.3. Multivariate Analysis of Total Quality (PCA)

To comprehensively evaluate the plasticity of the berry in response to environmental stress, a Principal Component Analysis (PCA) was performed using the orthogonal continuous quality variables, excluding the mathematically derived Maturity Index. The first two dimensions of the model (PC1 and PC2) accounted for 71.0% of the total biological variance.

The biplot analysis (Figure 2) revealed that chemical traits and biomechanical/colorimetric variables drive the phenotype in opposite directions. The variable loadings indicate that PC1 is primarily driven by colorimetric coordinates (L^* and b^*) and total soluble solids (TSS), while PC2 is strongly associated with epidermal firmness and titratable acidity (TA). The spatial distribution of the sample scores demonstrates that the bagged cohorts exhibit a consistent vectorial migration associated with lower instrumental resistance and stable colorimetric coordinates. In contrast, the spatial dispersion driven by primary metabolism vectors underscores that internal ripening dynamics remain highly sensitive to environmental and varietal fluctuations.

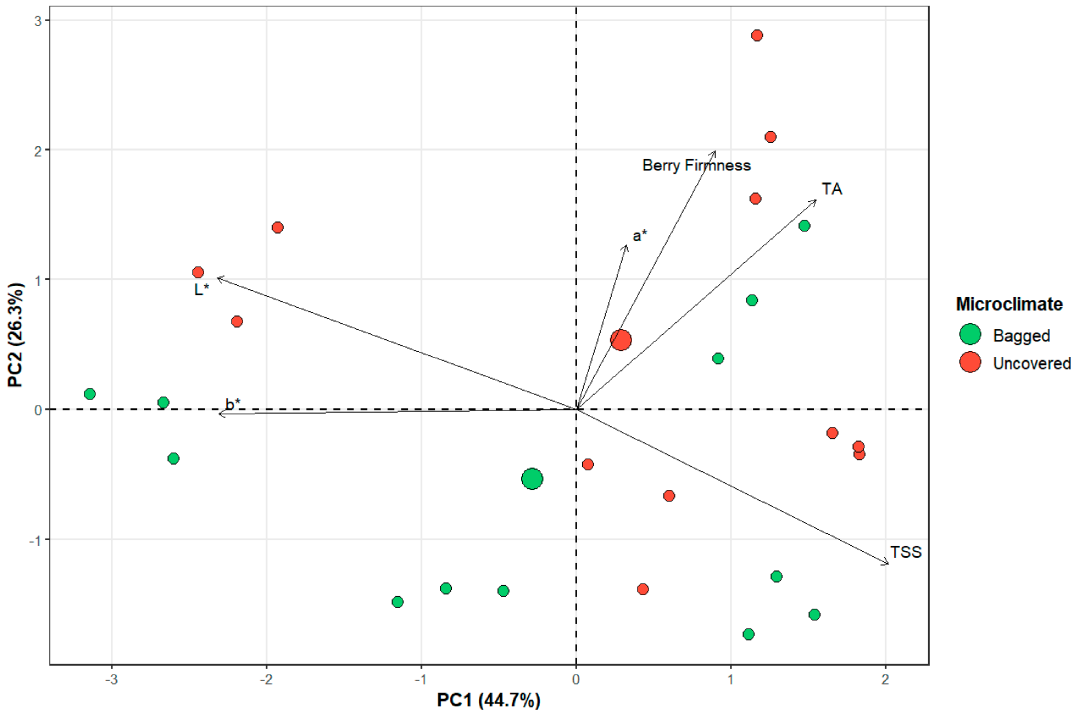


Figure 2. Principal Component Analysis (PCA) biplot of the physicochemical and biomechanical parameters. The axes represent PCA 1 and PCA 2, capturing the majority of the total dataset variance. The Maturity Index was excluded from the matrix to avoid structural collinearity. Points represent the individual experimental units (n = 3 clusters per group), color-coded by microclimate treatment (Bagged vs. Uncovered). Confidence ellipses were omitted to prevent unstable inferences.

4. Discussion

4.1. Preserved Biomechanical Modulation: The Impact of the Microclimate

This study was designed to determine the effect of light exclusion on table grapes under conditions of high interannual variability. The results show that the bagging technique reduced maximum epidermal force to varying degrees, exhibiting a consistent trend across the cultivars analyzed ("Aledo" and "Doña María"). However, caution is warranted when extrapolating the analysis of this biomechanical modulation to the species level. Comparative studies have shown that the textural response is strongly influenced by genotype, while seedless cultivars frequently experience an increase in pulp hardness [21], seed-bearing varieties exhibit opposite patterns under light exclusion [7].

Despite this divergence in the pulp, the literature supports a highly convergent pattern in the exocarp (skin), where the breaking strength tends to decrease across the board [7,22]. These textural changes are consistent with cell wall remodeling processes, in which firmness is associated with variations in pectins and the activity of hydrolytic enzymes such as galactosidases during ripening [23–25]. We hypothesize that the microclimate created by the pouch inhibits photodegradation and excessive lignification of the epicuticular waxes [26]. By blocking direct sunlight, the fruit does not need to thicken its cellular epidermis as a mechanical defense barrier, resulting in a berry with lower instrumental puncture resistance but a more commercially standardized texture.

Beyond epidermal biomechanics, it is noteworthy that light exclusion induced a divergent physiological response regarding final berry weight. While 'Doña María' experienced a consistent increase in weight under the bags, 'Aledo' exhibited a decrease across both seasons (Table 1). This differential behavior suggests that the modified microclimate interacts specifically with the hydraulic architecture and the final stages of mesocell expansion of each cultivar. Such genotypic divergence in water and assimilate accumulation under

shading represents a complex physiological trait that warrants targeted eco-physiological investigation in future studies.

4.2. Colorimetric Stability and Multivariate Analysis

Principal Component Analysis (PCA) confirmed the dissociation between climatic instability and physical phenotype. The model demonstrated that light exclusion acted as the dominant driving force on lightness (L^*) and chromaticity coordinates, grouping the bagged berries into a consistent spatial cluster. This phenotypic convergence is consistent with previous research, which indicates that the interception of sunlight delays veraison and downregulates the biosynthesis of photoprotective compounds [10,27]. Specifically, light exclusion suppresses the expression of key genes in the phenylpropanoid pathway, limiting the accumulation of flavonols and anthocyanins in grape skin [28].

Berry lightening is not merely a superficial phenomenon, but rather the visible expression of a metabolic reprogramming that stabilizes the CIELAB color space, neutralizing the variations that direct exposure to sunlight would typically induce [29,30]. Furthermore, it is important to note that the magnitude of this effect depends on the photoselective properties of the bag material [31].

4.3. Limitations and Agronomic Significance

It is critical to note that the internal bag microclimate parameters were not continuously logged; therefore, physiological mechanisms regarding light interception and wax lignification discussed herein are inferred based on the observed macroscopic phenotype and established literature rather than direct micro-environmental measurement. While this macroscopic phenotypic assessment clearly demonstrates the environmental buffering capacity of the bagging microclimate, it is important to strictly distinguish measured outcomes from hypothesized cellular mechanisms. The observed reduction in epidermal firmness strongly suggests a downregulation of cell wall lignification and cuticular wax thickening; however, specific transcriptomic, enzymatic (e.g., galactosidase activity), and comprehensive cell wall compositional analyses were beyond the scope of this study. Furthermore, the lack of quantitative data on the dynamics of volatile compounds limits our understanding of the full organoleptic profile. Future research should integrate multi-omics approaches to fully elucidate the molecular underpinnings of this mechanically consistent, yet metabolically plastic, phenotype within these cultivars.

Despite the robustness of the factorial design used—based on orthogonal sampling of representative cohorts—the scope of this study has certain inherent limitations. Because this is a macroscopic phenotypic assessment, the design does not allow for the elucidation of the precise transcriptional mechanisms underlying the loss of firmness [32]. Furthermore, we lack quantitative data on the dynamics of volatile compounds, which are often affected by this microclimate [33]. A critical methodological limitation of this study is the inherent confounding effect between the cultivar and the duration of light exclusion. Because ‘Doña María’ and ‘Aledo’ possess distinct phenological cycles, their respective bagging durations (70–75 days versus 120 days) were inextricably linked to their genetic background. Consequently, any observed genotypic interaction cannot be entirely isolated from the physical exposure time. Future experimental designs should consider analyzing bagging duration as a continuous covariate to decouple these interacting phenomena.

However, the agronomic implications are substantial. In the current context of global warming, viticulture faces highly unpredictable harvest quality due to the impact of extreme heat stress, which forces the berry to drastically remodel its metabolic profile to maintain cellular integrity [34,35]. This study provides multi-year empirical evidence that pre-harvest bagging exerts a strong buffering effect against thermal stress. By modifying the immediate

microclimate, the technique mitigates the phenotypic variation in texture. Although there is an inherent trade-off involving delayed ripening and color loss [36], bagging ensures that growers achieve a biomechanically predictable, resilient crop with high commercial uniformity, even during periods of abnormal heat stress.

5. Conclusions

Pre-harvest bagging acts as a unifying microclimate that consistently and predictably reduces epidermal puncture force (firmness). This biomechanical response is robust and consistent across the studied cultivars ('Aledo' and 'Doña María') and seasons. However, direct univariate statistics demonstrate that bagging does not universally stabilize color; parameters such as Lightness (L^*) and Hue angle present highly significant third-order interactions ($p < 0.05$), indicating a plastic response dependent on genotype and climate.

In direct contrast to the physical phenotype, technological maturity (TSS, acidity, and maturity index) exhibits highly interactive and genotype-dependent behavior (evidenced by highly significant third-order interactions, $p < 0.001$). This demonstrates that the internal dynamics of sugars and acids remain highly sensitive to the thermal severity of the year and to the variety.

Pre-harvest bagging emerges as a highly viable climate adaptation strategy for the studied cultivars. Although it involves a trade-off in the rate of ripening, it facilitates a more biomechanically predictable harvest with high commercial uniformity, significantly mitigating environmental variability in texture even under conditions of severe thermal stress in semi-arid regions.

Author Contributions: Conceptualization, N.T.C.M., E.S. and F.H.; formal analysis, N.T.C.M.; investigation, E.S. and F.H.; resources, E.S. and F.H.; writing—original draft preparation, N.T.C.M.; writing—review and editing, E.S. and F.H.; supervision, E.S. and F.H.; project administration, E.S. and F.H.; funding acquisition, E.S. and F.H. All authors have read and agreed to the published version of the manuscript.

Funding: Project AICO/2021/326 financed by the Autonomous Community of the Comunidad Valenciana through Conselleria de Innovación, Universidades, Ciencia y Sociedad Digital.

Data Availability Statement: The original contributions presented in this study are included in the article. Further inquiries can be directed to the corresponding authors.

Acknowledgments: The authors thank the Protected Designation of Origin (PDO) 'Uva de Mesa Embolsada del Vinalopó' for their support, and J. A. Martínez Cazorla, the owner of the vineyards, for his assistance.

Conflicts of Interest: The authors declare no conflicts of interest.

Abbreviations

The following abbreviations are used in this manuscript:

ANOVA	Analysis of Variance
CIAGRO-UMH	Institute for Agri-Food and Agri-Environmental Research and Innovation
CIELAB	Commission Internationale de l'Éclairage Color Space
ETRS89	European Terrestrial Reference System 1989
GIAS	Grupo de Investigación Agricultura Sostenible
PCA	Principal Component Analysis
PDO	Protected Designation of Origin
SD	Standard Deviation
TA	Titratable Acidity
TSS	Total Soluble Solids
UTM	Universal Transverse Mercator

References

1. Coronel Montesdeoca, N.T.; Andreu-Coll, L.; Jácome Sarchi, G.A.; Hernández, F.; Sendra, E. Fatty Acid Profile of Table Grapes: Impact of Cultivar and Fruit Protection on Saturated, Monounsaturated, and Polyunsaturated Fatty Acid Profile. *Foods* **2026**, *15*, 1585. [CrossRef] [PubMed]
2. Kiran, A.S.; Kavitha, C.; Soorianathasundaram, K.; Sritharan, N. Impact of Fruit Bagging with Different Coloured Non-woven Polypropylene Bags on Yield Attributes in Grapes. *Asian J. Dairy Food Res.* **2020**, *39*, 359–362. [CrossRef]
3. Venios, X.; Korkas, E.; Nisiotou, A.; Banilas, G. Grapevine Responses to Heat Stress and Global Warming. *Plants* **2020**, *9*, 1754. [CrossRef] [PubMed]
4. Rogiers, S.Y.; Greer, D.H.; Liu, Y.; Baby, T.; Xiao, Z. Impact of climate change on grape berry ripening: An assessment of adaptation strategies for the Australian vineyard. *Front. Plant Sci.* **2022**, *13*, 1094633. [CrossRef] [PubMed]
5. Sun, R.-Z.; Cheng, G.; Li, Q.; Zhu, Y.-R.; Zhang, X.; Wang, Y.; He, Y.-N.; Li, S.-Y.; He, L.; Chen, W.; et al. Comparative physiological, metabolomic, and transcriptomic analyses reveal developmental stage-dependent effects of cluster bagging on phenolic metabolism in Cabernet Sauvignon grape berries. *BMC Plant Biol.* **2019**, *19*, 583. [CrossRef] [PubMed]
6. Luca, L.P.; Scollo, F.; Distefano, G.; Ferlito, F.; Bennici, S.; Inzirillo, I.; Gentile, A.; La Malfa, S.; Nicolosi, E. Pre-Harvest Bagging of Table Grapes Reduces Accumulations of Agrochemical Residues and Increases Fruit Quality. *Agriculture* **2023**, *13*, 1933. [CrossRef]
7. Pisciotta, A.; Planeta, D.; Giacosa, S.; Paissoni, M.A.; Di Lorenzo, R.; Rolle, L. Quality of grapes grown inside paper bags in mediterranean area. *Agronomy* **2020**, *10*, 792. [CrossRef]
8. Andreu-Coll, L.; Blaya-Ros, P.J.; García-Castellanos, B.; Vigueras-Fernández, J.; Morales-Guevara, D.; García-García, J.; García-Brunton, J.; Calín-Sánchez, Á.; Hernández, F.; Galindo, A. Deficit Irrigation and Preharvest Chitosan Sprays Enhance Fruit Quality and Postharvest Performance in Peach. *Agronomy* **2026**, *16*, 361. [CrossRef]
9. Nahüel, C.G.; Martínez, L.; Nahüel, E.; Lázaro, H.; Castro, P. Impact of asymmetrical west-side canopy shading with anti-hail nets on vineyard microclimate, yield and wine composition. *Ciência Téc. Vitiv.* **2026**, *41*, 47–59. [CrossRef]
10. Li, M.-Y.; Li, H.-Q.; Deng, J.-Y.; Lu, H.-C.; Tian, M.-B.; Shi, N.; Wei, J.-Y.; He, F.; Yu, K.; Lan, Y.-B.; et al. Cluster bagging modifies flavonoid profiles in teinturier grape Garnacha Tintorera: Tissue-specific responses under different cultivation environments. *Food Chem.* **2026**, *38*, 104284. [CrossRef] [PubMed]
11. Wang, X.-Y.; Wang, H.-L.; Zhang, G.-J.; Yan, A.-L.; Ren, J.-C.; Liu, Z.-H.; Xu, H.-Y.; Sun, L. Effects of Fruit Bagging Treatment with Different Types of Bags on the Contents of Phenolics and Monoterpenes in Muscat-Flavored Table Grapes. *Horticulturae* **2022**, *8*, 411. [CrossRef]
12. Zhao, X.; Chen, S.; Wang, Z.; Lam, H.-M. Precision engineering of carbon partitioning enhances crop resilience to heat stress. *New Crops* **2026**, *3*, 100086. [CrossRef]
13. Liu, J.; Jin, W. Molecular underpinnings of plant stress granule dynamics in response to high-temperature stress. *New Crops* **2025**, *2*, 100069. [CrossRef]
14. Zhang, F.; Zeng, Y.; Guo, X.; Wang, J.; Zhou, Y.; Shang, B.; Zhang, X. The GhNAC091-GhZAT12 module regulates cotton acclimation to excess light via ROS scavenging. *New Crops* **2026**, *3*, 100085. [CrossRef]
15. Andreu-Coll, L.; García-Pastor, M.E.; Valero, D.; Amorós, A.; Almansa, M.S.; Legua, P.; Hernández, F. Influence of Storage on Physiological Properties, Chemical Composition, and Bioactive Compounds on Cactus Pear Fruit (*Opuntia ficus-indica* (L.) Mill.). *Agriculture* **2021**, *11*, 62. [CrossRef]
16. McGuire, R.G. Reporting of Objective Color Measurements. *HortScience* **1992**, *27*, 1254–1255. [CrossRef]
17. Andreu-Coll, L.; Noguera-Artiaga, L.; Sendra, E.; Hernández, F. Impact of Preharvest Bagging on the Volatile Profile of Vinalopó Table Grapes. *Agronomy* **2025**, *15*, 1066. [CrossRef]
18. R Core Team. *R: A Language and Environment for Statistical Computing*; R Foundation for Statistical Computing [Internet]: Vienna, Austria, 2024. Available online: https://www.r-project.org/ (accessed on 18 August 2026).
19. Fox, J.; Weisberg, S. *An R Companion to Applied Regression [Internet]*; SAGE Publications, Inc.: Thousand Oaks, CA, USA, 2018. Available online: https://www.sagepub.com/shop/buy-a-book/an-r-companion-to-applied-regression-3-246125 (accessed on 18 August 2026).
20. Lê, S.; Josse, J.; Husson, F. FactoMineR: An R Package for Multivariate Analysis. *J. Stat. Softw.* **2008**, *25*, 1–18. [CrossRef]
21. Naik, P.P.; Padashetti, B.; Hiremath, V.; Awati, M.; Gurupadappa Nanjappanavar, A.; Haveri, N. Influence of Preharvest Fruit Bagging on Quality, Disease and Pest Incidence in Grape (*Vitis vinifera* L.) cv. 'Crimson Seedless'. *Appl. Fruit. Sci.* **2026**, *68*, 61. [CrossRef]
22. Scalzini, G.; Vernhet, A.; Carillo, S.; Roi, S.; Véran, F.; Jørgensen, B.; Hansen, J.; Giacosa, S.; Segade, S.R.; Paissoni, M.A.; et al. Cell wall polysaccharides, phenolic extractability and mechanical properties of Aleatico winegrapes dehydrated under sun or in controlled conditions. *Food Hydrocoll.* **2024**, *149*, 109605. [CrossRef]
23. Balic, I.; Ejsmentewicz, T.; Sanhueza, D.; Silva, C.; Peredo, T.; Olmedo, P.; Barros, M.; Verdonk, J.C.; Paredes, R.; Meneses, C.; et al. Biochemical and physiological study of the firmness of table grape berries. *Postharvest Biol. Technol.* **2014**, *93*, 15–23. [CrossRef]

24. Balic, I.; Olmedo, P.; Zepeda, B.; Rojas, B.; Ejsmentewicz, T.; Barros, M.; Aguayo, D.; Moreno, A.A.; Pedreschi, R.; Meneses, C.; et al. Metabolomic and biochemical analysis of mesocarp tissues from table grape berries with contrasting firmness reveals cell wall modifications associated to harvest and cold storage. *Food Chem.* **2022**, *389*, 133052. [CrossRef] [PubMed]
25. Fuentes, S.; Fenoll, J.; Cava, J.; Garrido, I.; Molina, M.V.; Flores, P.; Hellín, P. Relationship between α- and β-galactosidase activities and firmness loss during the development of *Vitis vinifera* L. grape berries. *Acta Hortic.* **2018**, *1194*, 419–424. [CrossRef]
26. Li, H.; Bai, Y.; Yang, Y.; Zheng, H.; Xu, X.; Li, H.; Wang, W.; Tao, J. Transcriptomic analyses reveal light-regulated anthocyanin accumulation in 'ZhongShan-HongYu' grape berries. *Sci. Hortic.* **2023**, *309*, 111669. [CrossRef]
27. Zha, Q.; Xi, X.J.; He, Y.; Jiang, A.L. Bagging Affecting Sugar and Anthocyanin Metabolism in the Ripening Period of Grape Berries. *Not. Bot. Horti Agrobot. Cluj-Napoca* **2019**, *47*, 1194–1205. [CrossRef]
28. Sun, L.; Li, S.; Tang, X.; Fan, X.; Zhang, Y.; Jiang, J.; Liu, J.; Liu, C. Transcriptome analysis reveal the putative genes involved in light-induced anthocyanin accumulation in grape 'Red Globe' (*V. vinifera* L.). *Gene* **2020**, *728*, 144284. [CrossRef] [PubMed]
29. Ma, Z.-H.; Li, W.-F.; Mao, J.; Li, W.; Zuo, C.-W.; Zhao, X.; Dawuda, M.M.; Shi, X.-Y.; Chen, B.-H. Synthesis of light-inducible and light-independent anthocyanins regulated by specific genes in grape 'Marselan' (*V. vinifera* L.). *PeerJ* **2019**, *7*, e6521. [CrossRef] [PubMed]
30. Zhang, H.; Fan, P.; Liu, C.; Wu, B.; Li, S.; Liang, Z. Sunlight exclusion from Muscat grape alters volatile profiles during berry development. *Food Chem.* **2014**, *164*, 242–250. [CrossRef] [PubMed]
31. Zhang, K.; Wang, W.; Xie, Y.; Cao, J.; Cao, H.; Wang, X.; Xi, Z. Effects of photoselective cluster bags on 'Yan 73' Teinturier grape skin, flesh and wine: From color, phenolics, antioxidation, aromas and sensory perspective. *Food Chem.* **2026**, *499*, 147326. [CrossRef] [PubMed]
32. Ejsmentewicz, T.; Balic, I.; Sanhueza, D.; Barria, R.; Meneses, C.; Orellana, A.; Prieto, H.; Defilippi, B.G.; Campos-Vargas, R. Comparative Study of Two Table Grape Varieties with Contrasting Texture during Cold Storage. *Molecules* **2015**, *20*, 3667–3680. [CrossRef] [PubMed]
33. He, L.; Xu, X.Q.; Wang, Y.; Vanderweide, J.; Sun, R.Z.; Cheng, G.; Chen, W.; Li, S.D.; Li, S.P.; Duan, C.Q.; et al. Differential influence of timing and duration of bunch bagging on volatile organic compounds in Cabernet Sauvignon berries (*Vitis vinifera* L.). *Aust. J. Grape Wine Res.* **2022**, *28*, 75–85. [CrossRef]
34. Tian, M.-B.; Lu, H.-C.; Shi, N.; Li, M.-Y.; Wei, J.-Y.; Deng, J.-Y.; Cheng, C.-F.; Li, S.-D.; He, F.; Duan, C.-Q.; et al. Afternoon shading delays ripening and modifies grape flavonoids and wine composition under natural heat stress in semi-arid regions. *Food Chem.* **2025**, *29*, 102831. [CrossRef] [PubMed]
35. Ramos, M.C.; Martínez de Toda, F. Influence of weather conditions and projected climate change scenarios on the suitability of Vitis vinifera cv. Carignan in Rioja DOCa, Spain. *Int. J. Biometeorol.* **2022**, *66*, 1067–1078. [CrossRef] [PubMed]
36. Zutahy, Y.; Lichter, A.; Kaplunov, T.; Lurie, S. Extended storage of 'Red Globe' grapes in modified SO_2 generating pads. *Postharvest Biol. Technol.* **2008**, *50*, 12–17. [CrossRef]

Disclaimer/Publisher's Note: The statements, opinions and data contained in all publications are solely those of the individual author(s) and contributor(s) and not of MDPI and/or the editor(s). MDPI and/or the editor(s) disclaim responsibility for any injury to people or property resulting from any ideas, methods, instructions or products referred to in the content.